SLAC-PUB-8824
BABAR-PROC-01/27
hep-ex/0105018
May, 2001

MEASUREMENT OF CHARMLESS HADRONIC B DECAYS BRANCHING FRACTION AT BABAR.

G.Cavoto
on behalf of the BaBar Collaboration
Universitá di Roma La Sapienza, Dipartimento di Fisica and INFN,
I-00185 Roma, Italy
E-mail: gianluca.cavoto@roma1.infn.it

Abstract

We present preliminary measurements of the branching fractions for charmless hadronic decays of B mesons into two-body final states with kaons, pions and a ϕ resonance. The measurements are based on a data sample of approximately 23 million $B\bar{B}$ pairs collected by the BaBar detector at the PEP-II asymmetric B Factory at SLAC.

Contributed to the Proceedings of the
36th Rencontres De Moriond On QCD And Hadronic Interactions
17-24 Mar 2001, Les Arcs, France

Stanford Linear Accelerator Center, Stanford University, Stanford, CA 94309

Work supported in part by Department of Energy contract DE-AC03-76SF00515.

Charmless hadronic final states play an important role in the study of *CP*-violation. In the Standard Model, all *CP*-violating phenomena are a consequence of a single complex phase in the Cabibbo-Kobayashi-Maskawa (CKM) quark-mixing matrix [1]. Measurements of the rates and *CP* asymmetries for B decays into the charmless final states $\pi\pi$ and $K\pi$ can be used to constrain the angles α [2] of the unitarity triangle. Decays containing a ϕ meson are interesting since they are dominated by $b \to s(d)\bar{s}s$ peguin diagram, with potential benefits to estimates of direct *CP*-violation effects. They also allow an independent measurement of $\sin 2\beta$.

We present preliminary measurements of the branching fractions for charmless hadronic decays of B mesons in the final states $\pi^+\pi^-$, $K^+\pi^-$, $K^+\pi^0$, $K^0\pi^+$, $K^0\pi^0$, ϕK^+, ϕK^0, and $\phi K^{*+}(892)$ [3]. The data sample used in these analyses consists of 22.57×10^6 $B\overline{B}$ pairs, collected at the PEP-II e^+e^- collider (SLAC) with the BaBar detector [4] .

Hadronic events are selected based on track multiplicity and event topology. We use only good quality tracks: tracks are identified as pions or kaons using the Cherenkov angle θ_c measured by a unique, internally reflecting Cherenkov ring imaging detector (DIRC). Candidate K^0_S mesons are reconstructed from pairs of oppositely charged tracks that form a well-measured vertex and have an invariant mass within 3.5 standard deviations (σ) of the nominal K^0_S mass [5]. Candidate photons are defined as showers in the EMC that have the expected lateral shape and are not matched to a track. Candidate π^0 mesons are formed from pairs of photons with an invariant mass within 3σ of the nominal π^0 mass. The π^0 candidates are then kinematically fitted with their mass constrained to the nominal π^0 mass. All tracks (except K^0_S daughters) are required to have good-quality θ_c measurements that are inconsistent with the expected value for a proton. Electrons are rejected based on specific ionization ($\mathrm{d}E/\mathrm{d}x$) in the DCH system, shower shape in the EMC, and the ratio of shower energy to track momentum.

Candidate B mesons are reconstructed in the various topologies: $h^+h'^-$, $h^+\pi^0$, $K^0_S h^+$, $K^0_S\pi^0$, ϕh^+, ϕK^0_S, and ϕK^{*+} where the symbols h and h' refer to π or K. For ϕ candidates, both tracks must be identified as kaons whose invariant mass must lie within a $\pm 30\,\mathrm{MeV}/c^2$ interval centered around ϕ mass. The selection of K^{*+} comprises $K^+\pi^0$ and $K^0_S\pi^+$ combinations within a $K\pi$ mass interval of $\pm 150\,\mathrm{MeV}/c^2$. A K^* helicity angle cut effectively requires π^0 momentum greater than $0.35\,\mathrm{GeV}/c$.

Candidate B mesons are selected exploiting the kinematic constraints provided by the $\Upsilon(4S)$ initial state: we define a energy-substituted mass m_{ES}, where $\sqrt{s}/2$ is substituted for candidate's energy, and the difference ΔE between the B-candidate energy and $\sqrt{s}/2$. For all modes the m_{ES} resolution is dominated by the beam energy spread and is approximately $2.5\,\mathrm{MeV}/c^2$, while ΔE resolution is mode dependent and dominated by momentum resolution. Candidates are selected in the range $5.2 < m_{\mathrm{ES}} < 5.3\,\mathrm{GeV}/c^2$. Candidates are accepted, depending on the decay topology, in various ΔE ranges, which are restrictive enough to suppress backgrounds due to other types of B decays.

The largest source of background is from random combinations of tracks and neutrals produced in the $e^+e^- \to q\overline{q}$ continuum (where $q = u$, d, s or c). In the CM frame this background typically exhibits a two-jet structure. In contrast, the low momentum and pseudoscalar nature of B mesons in the decay $\Upsilon(4\mathrm{S}) \to B\overline{B}$ leads to a more spherically symmetric event. This topology difference is exploited using two event-shape quantities: the angle θ_S [6] between the sphericity axes, evaluated in the CM frame, of the B candidate and the remaining tracks and photons in the event. The distribution of the absolute value of $\cos\theta_S$ is strongly peaked near 1 for continuum events and is approximately uniform for $B\overline{B}$ events. We require $|\cos\theta_S| < 0.9$

The second quantity used in the analyses is a Fisher discriminant $\mathcal{F}$ which consists of a linear

combination of several variables that distinguish signal from background [7]. The experimental observables used in the definition of $\mathcal{F}$ are the scalar sum of the momenta of all tracks and photons (excluding the B candidate daughters) flowing into nine concentric cones centered on the thrust axis of the B candidate, in the CM frame. Each cone subtends an angle of 10° and is folded to combine the forward and backward intervals.

The global detection efficiencies, which include the intermediate particle branching fractions, are listed in Table 1.

Table 1: Summary of results for detection efficiencies (ϵ), numbers of fitted signal yields (N_S), statistical significances, and measured branching fractions ($\mathcal{B}$). (90% confidence level upper limits). The efficiencies include the branching fractions for $K^0 \to K^0_S \to \pi^+\pi^-$, $\pi^0 \to \gamma\gamma$, $\phi \to K^+K^-$. Equal branching fractions for $\Upsilon(4S) \to B^0\overline{B}^0$ and B^+B^- are assumed.

Mode	ϵ (%)	N_S	Stat. Sig. (σ)	$\mathcal{B}(10^{-6})$
$\pi^+\pi^-$	45	41 ± 10	4.7	$4.1 \pm 1.0 \pm 0.7$
$K^+\pi^-$	45	169 ± 17	15.8	$16.7 \pm 1.6 \pm 1.3$
K^+K^-	43	$8.2^{+7.8}_{-6.4}$	1.3	< 2.5
$\pi^+\pi^0$	32	37 ± 14	3.4	< 9.6
$K^+\pi^0$	31	75 ± 14	8.0	$10.8^{+2.1}_{-1.9} \pm 1.0$
$K^0\pi^+$	14	59^{+11}_{-10}	9.8	$18.2^{+3.3}_{-3.0} \pm 1.7$
$\overline{K}^0K^+$	14	$0.0^{+2.4}_{-0}$	0	< 2.5
$K^0\pi^0$	9.6	$17.9^{+6.8}_{-5.8}$	4.5	$8.2^{+3.1}_{-2.7} \pm 1.1$
ϕK^+	18	$31.4^{+6.7}_{-5.9}$	10.5	$7.7^{+1.6}_{-1.4} \pm 0.8$
$\phi\pi^+$	19	$0.9^{+2.1}_{-0.9}$	0.6	< 1.4
ϕK^0	6	$10.8^{+4.1}_{-3.3}$	6.4	$8.1^{+3.1}_{-2.5} \pm 0.8$
ϕK^{*+}	5		4.5	$9.7^{+4.2}_{-3.4} \pm 1.7$
$\phi K^{*+}_{K^+}$	2.5	$7.1^{+4.3}_{-3.4}$	2.7	$12.8^{+7.7}_{-6.1} \pm 3.2$
$\phi K^{*+}_{K^0}$	2.4	$4.4^{+2.7}_{-2.0}$	3.6	$8.0^{+5.0}_{-3.7} \pm 1.3$

Signal yields are determined from an unbinned maximum likelihood fit using $m_{\rm ES}$, ΔE, $\mathcal{F}$, θ_c, ϕ mass, and K^{*+} mass (where applicable). In each of the fits, the likelihood for a given candidate j is obtained by summing the product of event yield n_k and probability $\mathcal{P}_k$ over all possible signal and background hypotheses k. The n_k are determined by maximizing the extended likelihood function $\mathcal{L}$:

$$\mathcal{L} = \exp\left(-\sum_{i=1}^{M} n_i\right) \prod_{j=1}^{N} \left[\sum_{k=1}^{M} n_k \mathcal{P}_k\left(\vec{x}_j; \vec{\alpha}_k\right)\right] . \tag{1}$$

where $\mathcal{P}_k(\vec{x}_j; \vec{\alpha}_k)$ is the probability for candidate j to belong to category k (of M total categories), based on its characterizing variables $\vec{x}_j$ and parameters $\vec{\alpha_k}$ that describe the expected distributions of these variables. The probabilities $\mathcal{P}_k(\vec{x}_j; \vec{\alpha}_k)$ are evaluated as the product of probability density functions (PDFs) for each of the independent variables $\vec{x}_j$, given the set of parameters $\vec{\alpha}_k$. Monte Carlo simulated data is used to validate the assumption that the fit variables are uncorrelated. The exponential factor in $\mathcal{L}$ accounts for Poisson fluctuations in the total number of observed events N.

The probabilities for each possible signal and background hypotheses are evaluated as the product of probability density functions (PDFs) for each of the independent variables. The parameters of $m_{\rm ES}$, ΔE, and $\mathcal{F}$ PDFs are determined from data, and are cross-checked with Monte Carlo

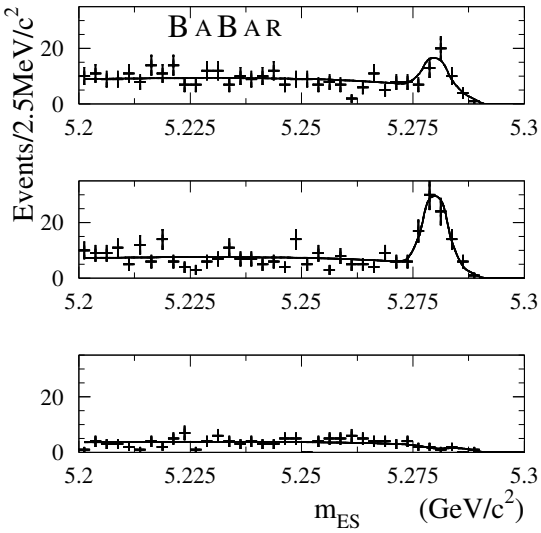

Figure 1: The $m_{\rm ES}$ distributions for candidates which are (from top to bottom) $\pi^+\pi^-$-like, $K^+\pi^-$-like, K^+K^--like The curves represent fits to the distributions

simulation. In particular, a sample of D^*-tagged $D^0 \to K^-\pi^+$ decays is used to parametrize the θ_C distribution for pion and kaon tracks as a function of momentum. The results of the fits for the various topologies are summarized in Table 1. We find evidence for the decay $B^+ \to \pi^+\pi^0$ and measure a branching fraction of $\mathcal{B}(B^+ \to \pi^+\pi^0) = (5.1^{+2.0}_{-1.8} \pm 0.8) \times 10^{-6}$. However, the signal significance is insufficient to claim observation. A 90% confidence level upper limit is computed for this mode, as well as for $B^0 \to K^+K^-$ $B^+ \to \overline{K}^0K^+$, and $B^+ \to \phi\pi^+$ in the following manner. The upper limit on the signal yield for mode k is given by the value of n_k^0 for which $\int_0^{n_k^0} \mathcal{L}_{\rm max}\, {\rm d}n_k / \int_0^\infty \mathcal{L}_{\rm max}\, {\rm d}n_k = 0.90$, where $\mathcal{L}_{\rm max}$ is the likelihood as a function of n_k, maximized with respect to the remaining fit parameters.

The result is then increased by the total systematic error. The detection efficiency is reduced by its systematic uncertainty in calculating the branching fraction upper limit. The statistical significance of a given channel is determined by fixing the yield to zero, repeating the fit, and recording the change in $-2\ln\mathcal{L}$.

Figure 1 shows the distributions in $m_{\rm ES}$ for events passing the selection criteria, as well as requirements on Fisher value, which are used to increase the relative fraction of signal events of a given type. Fits to these distributions are overlaid.

Imperfect knowledge of the PDF shapes and of the detection efficiencies are the main sources of systematic uncertainties on the branching ratio measurements. Uncertainties in the PDF parameterizations are estimated either by varying the PDF parameters within 1σ of their measured uncertainties or by substituting alternative PDF from independent control samples, and recording the variations in the fit results.

In summary, we have measured branching fractions for the rare charmless decays $B^0 \to \pi^+\pi^-$, $B^0 \to K^+\pi^-$, $B^+ \to K^+\pi^0$, $B^+ \to K^0\pi^+$, $B^0 \to K^0\pi^0$, ϕK^+, ϕK^0, and ϕK^{*+} and set upper limits on $B^0 \to K^+K^-$, $B^+ \to \pi^+\pi^0$, $B^+ \to \overline{K}^0K^+$, and $\phi\pi^+$.

Acknowledgments

This work has been supported by the US Department of Energy and National Science Foundation, the Natural Sciences and Engineering Research Council (Canada), the Institute of High Energy Physics (China), Commissariat à l'Energie Atomique and Institut National de Physique Nucléaire et de Physique des Particules (France), Bundesministerium für Bildung and Forschung (Germany), Istituto Nazionale di Fisica Nucleare (Italy), the Research Council of Norway, the Ministry of Science and Technology of the Russian Federation and the Particle Physics and Astronomy Research Council (United Kingdom).

References

1. N. Cabbibo, Phys. Rev. Lett. **10**, 531 (1963); M. Kobayashi and T. Maskawa, Prog. Theor. Phys. **49**, 652 (1973).
2. M. Gronau and D. London, Phys. Rev. Lett. **65**, 3381 (1990); M. Gronau, J.L. Rosner and D. London, Phys. Rev. Lett. **73**, 21 (1994); R. Fleischer, Phys. Lett. B **365**, 399 (1996); R. Fleischer and T. Mannel, Phys. Rev. D **57**, 2752 (1998); M. Neubert and J. Rosner, Phys. Lett. B **441**, 403 (1998); M. Neubert, J. High Energy Phys. **02**, 014 (1999).
3. Charge conjugate states are assumed throughout, except where explicitly noted.
4. BaBar collaboration, B. Aubert *et al.*, SLAC-PUB-8569, submitted to Nucl. Instr. and Methods **.**
5. Particle Data Group, D.E. Groom *et al.*, Eur. Phys. Jour. C **15**, 1 (2000).
6. S.L. Wu, Phys. Rep. **107**, 59 (1984).
7. CLEO collaboration, D.M. Asner *et al.*, Phys. Rev. D **53**, 1039 (1996).